DOI: 10.1111/cgf.12524

COMPUTER GRAPHICS *forum*
Volume 00 (2014), number 0 pp. 1–12

Optimization-Based Gradient Mesh Colour Transfer

Yi Xiao[1,2], Liang Wan[3,*], Chi Sing Leung[2], Yu-Kun Lai[4] and Tien-Tsin Wong[5]

[1]Hunan University, Changsha, China
yixiao1984@gmail.com
[2]City University of Hong Kong, Hong Kong SAR, China
eeleungc@cityu.edu.hk
[3]Tianjin University, Tianjin, China
lwan@tju.edu.cn
[4]Cardiff University, Cardiff CF10 3AT, UK
yukun.lai@cs.cardiff.ac.uk
[5]The Chinese University of Hong Kong; CUHK Shenzhen Research Institute, China
ttwong@cse.cuhk.edu.hk

Abstract

In vector graphics, gradient meshes represent an image object by one or more regularly connected grids. Every grid point has attributes as the position, colour and gradients of these quantities specified. Editing the attributes of an existing gradient mesh (such as the colour gradients) is not only non-intuitive but also time-consuming. To facilitate user-friendly colour editing, we develop an optimization-based colour transfer method for gradient meshes. The key idea is built on the fact that we can approximate a colour transfer operation on gradient meshes with a linear transfer function. In this paper, we formulate the approximation as an optimization problem, which aims to minimize the colour distribution of the example image and the transferred gradient mesh. By adding proper constraints, i.e. image gradients, to the optimization problem, the details of the gradient meshes can be better preserved. With the linear transfer function, we are able to edit the colours and colour gradients of the mesh points automatically, while preserving the structure of the gradient mesh. The experimental results show that our method can generate pleasing recoloured gradient meshes.

Keywords: gradient mesh, example-based colour transfer, linear operator, optimization

ACM CCS: I.3.3 [Computer Graphics]: Picture/Image Generation—

1. Introduction

In vector graphics, the gradient mesh, offered by Adobe Illustrator and Coreldraw, is a popular representation, which is suitable for representing multi-coloured objects with smoothly varying colours. It is used to create photo-realistic vector art by many artists. Gradient meshes represent an image object by one or more regularly connected grids. Every grid point (also called a control point) has attributes including the position, colour and gradients of these quantities defined in the parametric domain. The image represented by gradient meshes is obtained by bicubic interpolation of the specified grid information.

To create gradient meshes, artists have to manually specify mesh grids and manipulate the associated attributes, which is labour intensive. The problem has gained attention such that several methods for (semi-)automatic generation of gradient meshes [SLWS07, LHM09] have been developed. Good results can be obtained with the aid of some user assistance. Although gradient meshes can be obtained automatically, how to *efficiently edit* gradient meshes remains problematic. Due to the large number of attributes associated with each control point, manually editing the attributes (such as the colour gradients) of an *existing gradient mesh*, which can be obtained by manual operation or automatic generation, is not only non-intuitive but also time-consuming. When the gradient mesh contains a large number of mesh points, or the vector art consists of multiple gradient meshes, it becomes especially important to have more convenient and efficient ways for gradient mesh editing.

A straightforward way to relieve the colour editing problem is to borrow the colour editing methods for raster images, such as colour transfer [RAGS01]. However, these methods cannot directly deal with gradient meshes, which have more attributes per element than raster images. People may consider performing colour transfer

*Corresponding author: Liang Wan (lwan@tju.edu.cn)

on the rasterized gradient mesh and then regenerating the gradient meshes from the recoloured rasterized gradient mesh using the methods in [SLWS07, LHM09]. Nevertheless, it should be pointed out that using the generation method in [SLWS07] or [LHM09] is an approximating process, which will result in loss of detail information in the recoloured image. While consuming extra computing time, the regeneration may also change the gradient mesh structure, which is important in some scenarios where the structure was originally obtained through labour-intensive manual creation or complicated optimization.

Considering these issues, in our previous work [XWL*13], we proposed a principal component analysis (PCA)-based linear colour transfer method, which changes the colour style of a gradient mesh by borrowing the colour statistics of an example image. This method investigates a nice property of a gradient mesh that applying a linear operator on the colour component is equivalent to applying the linear operator on the colours and colour gradients of the control points, respectively. The linear operator is defined as a fused version of two basic PCA-based colour transfer algorithms [XM06, AK07]. We call this method PCA Fusion [XWL*13]. Although this method can obtain pleasing results in most cases, there still exist some disadvantages that can be further improved. The PCA Fusion method implicitly assumes that the colours of the example image and the gradient mesh are Gaussian distributed, and only matches their means and variances in the decorrelated colour space. Unfortunately, since the mean and variance are global properties, matching only them may result in out-of-gamut artefacts, which means some colours in the recoloured gradient mesh may not be present in the example image. Moreover, the PCA Fusion method does not consider preserving the detail information represented in the gradient mesh such as highlights and textures, which may be destroyed after colour transfer. Finally, the PCA Fusion method may incur colour inconsistency artefacts because of the fusion operation.

In this paper, we propose a novel framework for gradient mesh colour transfer to edit gradient meshes. The key insight of our framework is to approximate a colour transfer operator with an *optimal* linear transfer function. The approximation can be well formulated as a classical minimization problem, which equivalently minimizes the differences between the colour distribution of the linear transferred gradient mesh and that of an example image. Although our current method also uses a linear transform, we use a totally different framework. In the previous work, the linear transform is defined by PCA, which implicitly assumes the colour distributions of the example image and the gradient mesh are Gaussian. In our current work, the transform is defined by directly minimizing the difference of colour distributions, which does not have such an assumption. Therefore, our current method handles images with non-Gaussian colour distributions, and also better matches the colours, so that the out-of-gamut colours are avoided. Moreover, in our current method, image gradients can be explicitly added to the minimization model as a constraint, which can control the influence of the transfer and preserve the details of the gradient mesh. Also, since the linear transform is solved directly from the minimization problem, artefacts due to the fusion operation in the previous work are avoided. Experimental results and a user study show that our method avoids abnormal colours caused by the unmatched distributions, and also better preserves the details of the gradient meshes. Figure 1 shows an example of the results obtained by our method.

2. Related Work

Colour transfer, first introduced by Reinhard *et al.* [RAGS01], refers to a category of methods which modify the colour distribution of a target image according to that of a reference image. Since its introduction, a large number of methods have been developed, and a recent survey can be found in [FPC*14]. Reinhard *et al.* [RAGS01] modelled the colour distribution of an image using the mean and standard deviation of colour values in $l\alpha\beta$ space, due to the colour correlation in RGB space. The mean and standard deviation of both the target image and the reference image are then used for shifting and scaling the colours of the pixels in the target image. This method was then extended to produce an image sequence based on multiple reference images and user input parameters [WH04].

Abadpour and Kasaei [AK07] decorrelated the colours in RGB space using PCA and then matched the means and standard deviations in the decorrelated space. The colour distribution is transferred to the target image by applying PCA-based transformation on each pixel. Similar ideas were also reported in [XM06, Kot05].

Instead of matching the mean and standard deviation, some global colour mapping techniques directly match the histograms [WSM99, MS03, GD05a, NN05]. Recently, Pouli and Reinhard [PR11] presented a histogram reshaping technique for images of arbitrary dynamic range. In these histogram matching methods, the colours are transformed to a colour space which is assumed to be uncorrelated, such as CIELab. The histogram of each colour channel is then matched separately. Alternatively, Pitie *et al.* [PKD07] cast a three-dimensional colour distribution matching problem into a sequence of one-dimensional matching problems via the Radon transform. This method is suitable for any colour spaces. The impact of colour spaces on colour transfer effects was recently exploited by Reinhard and Pouli [RP11].

Greenfield and House [GH03] performed image segmentation, and extracted a colour palette by choosing representative colours from the segments. The colour mapping between the palettes of the reference and target images is then computed. Rather than binary segmentation, Tai *et al.* [TJT05] applied probabilistic segmentation that produces soft region boundaries. Chang *et al.* [CSN03] categorized each pixel as one of the 11 basic perceptual colour categories. Then, colour transformation was applied within the same basic colour category. This method has been extended to video data [CSN07]. Dong *et al.* [DBZP10] defined a one-to-one mapping between two dominant colour sets, which are extracted from both the target image and reference image using probabilistic segmentation. The mapped dominant colours are then used for transforming the pixels in the target image. Wu *et al.* [WDM*11] adopted this idea and they further proposed to preserve the spatial distribution of the dominant colours. Su *et al.* [SDYL12] decomposed the target image into the base and detail layers. The colours of base layers are mapped by matching the distribution of base layers and that of a reference image. The final result is produced by combining the mapped base layers with the detail layers.

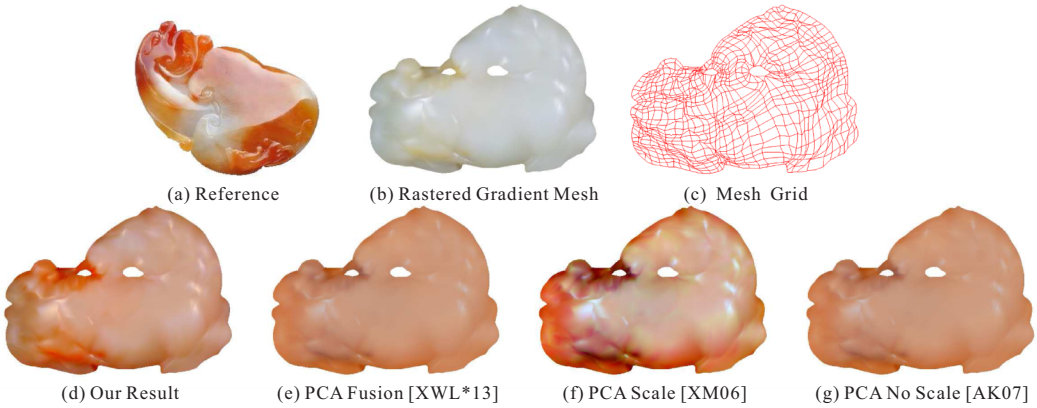

Figure 1: *Results of the jade example. Our method faithfully captures the colour style of the example image and better preserves the details of the gradient meshes. λ is set to 1 in this example.*

To avoid the spatially inconsistent artefacts caused by some per pixel operations like histogram matching, Pitie *et al.* [PKD07] suggested recovering the details of the target image after the per pixel operation. This is done by preserving the original gradients in the target image. Similar ideas can also be found in [LWX07, WHCO08, XM09, DBZP10], although expressed in different formulations. Instead of preserving gradient, Grundland and Dodgson proposed mapping reference colour gradients to corresponding target colour gradients [GD05b]. In our new method, by comparison, we use the gradient term as a constraint in the optimization process.

The aforementioned methods can produce pleasing results when the colour distributions of the reference and target images are homogeneous. Otherwise, they can generate unnatural looking results. To address this problem, some researchers suggested relying on user input swatches pairs to classify the colours [RAGS01, WAM02, XM06, AK07, AP10]. The colour transfer is then locally performed within each swatch pair. The final colour is the weighted sum of the results from all swatch pairs. In our method, we adopt this idea. We define a linear operator for each pair of swatches, and combine the linear transformed colours and colour derivatives of all pairs.

Inspired by Reinhard *et al.*'s work [RAGS01], Welsh *et al.* [WAM02] colourized a greyscale image by borrowing the colour characteristics of a colour reference image.

Instead of using a reference image, Levin *et al.* [LLW04] allowed users to specify the reference colour distributions by drawing colour strokes over a greyscale image. They then proposed a global optimization method to diffuse colour strokes across the entire greyscale image. There have been many attempts to improve the computational efficiency of this process [HK05, HTC*05, ICOL05, YS06, LWCO*07]. In addition, automatic greyscale image colourization methods have been developed [JLWT04, CHS08, LHZ08, MTN09].

3. Gradient Mesh

We now describe the mathematical representation of gradient meshes and discuss its linear property.

3.1. Gradient mesh representation

As defined in [SLWS07, LHM09], a gradient mesh is a topologically planar rectangular grid, whose every four nearby control points (vertices) define a primitive component called a Ferguson patch [Fer64]. Figure 2 shows a gradient mesh with four Ferguson patches. For each control point in the grid, three types of information are specified: position $\mathbf{p} = (x, y)$, colour $\mathbf{c} = (r, g, b)$ and their gradients $\mathbf{p}_u, \mathbf{p}_v, \mathbf{c}_u, \mathbf{c}_v$. Note that the gradients are defined in parametric coordinate space u, v, where $0 \le u, v \le 1$. Each Ferguson patch in the gradient mesh is rendered via bicubic Hermite interpolation, given by

$$m(u, v) = \mathbf{u} C Q C^T \mathbf{v}^T, \tag{1}$$

where

$$Q = \begin{bmatrix} m^0 & m^2 & m^0_v & m^2_v \\ m^1 & m^3 & m^1_v & m^3_v \\ m^0_u & m^2_u & 0 & 0 \\ m^1_u & m^3_u & 0 & 0 \end{bmatrix},$$

$$C = \begin{bmatrix} 1 & 0 & 0 & 0 \\ 0 & 0 & 1 & 0 \\ -3 & 3 & -2 & -1 \\ 2 & -2 & 1 & 1 \end{bmatrix},$$

m can be any of x, y, r, g, b, the superscript of m indicates one of the four control points of the Ferguson patch, $\mathbf{u} = [1\ u\ u^2\ u^3]$, $\mathbf{v} = [1\ v\ v^2\ v^3]$ and the parameters have the range of $0 \le u, v \le 1$. Given a parameter pair (u, v), its position and colour are calculated using the above equation.

Since the position $\mathbf{p} = (x, y)$ and the colour component $\mathbf{c} = (r, g, b)$ are given in parametric space, (1) implicitly defines a function $\mathbf{c} = \mathbf{g}(x, y, \mathbf{p}^i, \mathbf{p}^i_u, \mathbf{p}^i_v, \mathbf{c}^i, \mathbf{c}^i_u, \mathbf{c}^i_v, i \in \Gamma)$, where i is the index of a control point, Γ is the set which contains all the indices of the control points. Since $\mathbf{p}^i, \mathbf{p}^i_u, \mathbf{p}^i_v, \mathbf{c}^i, \mathbf{c}^i_u, \mathbf{c}^i_v, i \in \Gamma$ are constant, $\mathbf{g}(\cdot)$ implicitly defines the mapping between position (x, y) and colour (r, g, b). Due to the complexity of (1), $\mathbf{g}(\cdot)$ cannot be expressed explicitly. To get a raster gradient mesh, we sample in the parametric domain

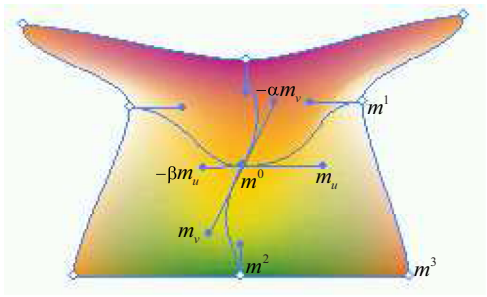

Figure 2: *The gradient mesh contains four Ferguson patches. The gradient information is illustrated for point m^0 in the bottom-right patch.*

(u, v) to get a raster image of the gradient mesh. This sampling process is called rasterization. Denote the rasterized gradient mesh as $\mathbf{c} = \mathbf{s}(x, y)$, the process of rasterization is denoted by $Ras(\cdot)$. Then, we have $\mathbf{s}(x, y) = Ras(\mathbf{g}(x, y, \mathbf{p^i}, \mathbf{p^i_u}, \mathbf{p^i_v}, \mathbf{c^i}, \mathbf{c^i_u}, \mathbf{c^i_v}, i \in \Gamma))$.

3.2. The linear property of gradient mesh

As pointed out in [XWL*13], gradient meshes are defined in a parametric domain and have curvilinear grid structures. Since the grid structures should be preserved during the transfer, we aim to perform colour editing in the parametric domain. In other words, we try to tackle colours and colour gradients of control points.

In [XWL*13], Xiao *et al.* investigated the linear property of the gradient mesh. They found that applying a linear operator on the colour component is equivalent to applying the linear operator on the colours and colour gradients of the control points. We summarize the linear property of the gradient mesh in matrix form. When applying a linear operator $L(\cdot)$ represented by a 3×3 matrix T and a 3×1 translation vector $\mathbf{b}$ on $\mathbf{m}(u, v)$, we get

$$T\mathbf{m}(u, v) + \mathbf{b} \rightarrow \begin{cases} T\mathbf{m}^i + \mathbf{b}, & \text{for } i = 0, 1, 2, 3, \\ T\mathbf{m}^i_u, & \text{for } i = 0, 1, 2, 3, \\ T\mathbf{m}^i_v, & \text{for } i = 0, 1, 2, 3, \end{cases} \tag{2}$$

where $\mathbf{m}(u, v) = [m_r(u, v), m_g(u, v), m_b(u, v)]^T$ is the colour vector at the parametric coordinate (u, v), $\mathbf{m}^i = [m^i_r, m^i_g, m^i_b]^T$ is the colour vector of the ith control point and $\mathbf{m}^i_u$, $\mathbf{m}^i_v$ are the colour derivatives of the ith control point. From the above equation, we can see that a linear operator is transparent to parametric interpolation. That is, if we want to linearly transform the colours inside a patch, we just need to perform the linear transformation on the colours and colour gradients of the four control points, and rerasterize the gradient mesh. The linear property can also be applied to the rasterized gradient mesh, which is given by

$$\begin{aligned} L(\mathbf{s}(x, y)) &= L(Ras(\mathbf{g}(x, y, \mathbf{p^i}, \mathbf{p^i_u}, \mathbf{p^i_v}, \mathbf{c^i}, \mathbf{c^i_u}, \mathbf{c^i_v}, i \in \Gamma))) \\ &= Ras(\mathbf{g}(x, y, \mathbf{p^i}, \mathbf{p^i_u}, \mathbf{p^i_v}, L(\mathbf{c^i}), T\mathbf{c^i_u}, T\mathbf{c^i_v}, i \in \Gamma)), \end{aligned} \tag{3}$$

where $L(\mathbf{c}) = T\mathbf{c} + \mathbf{b}$. The advantage of this property is twofold. First, a linear operator can be defined using the rasterized gradient mesh, whose statistical and other properties can be more easily calculated. Second, the computational cost of the linear transformation only depends on the gradient mesh size, which is much smaller than the resolution of the rasterized gradient mesh in general. Note that the position information $\mathbf{p^i}$, $\mathbf{p^i_u}$, $\mathbf{p^i_v}$ are preserved, we ignore them in the following expressions. Meanwhile, we use $\mathbf{g}(x, y, L(\cdot))$ to denote $\mathbf{g}(x, y, L(\mathbf{c^i}), T\mathbf{c^i_u}, T\mathbf{c^i_v}, i \in \Gamma)$ to simplify the expression.

4. Optimization-Based Colour Transfer

4.1. Single-swatch colour transfer

The purpose of colour transfer is to edit the gradient mesh so that the edited gradient mesh has a similar colour distribution to an example image, while preserveing the details of the gradient mesh. Therefore, we need to measure the colour distribution function and the details of the gradient mesh. Since the colour distribution function cannot be analytically derived, we use the cumulative distribution function of the rasterized image obtained from the gradient mesh as in [XWL*13]. The details of the gradient mesh are measured by the image gradients of the rasterized image as in [PKD07, XM09]. We first consider a simple case in which the gradient mesh is to borrow the colour distribution from the whole image. Considering the two purposes of colour transfer, we formulate the colour transfer process as a minimization model including two terms, one to measure the difference of the colour distribution functions, and the other to measure the modification in image gradients. The minimization model is given by

$$E = \arg\min_L E_1 + \lambda E_2, \tag{4}$$

where

$$\begin{aligned} E_1 &= \int_\Omega \| cdf^{Ras(\mathbf{g}(x,y,L(\cdot)))}(\mathbf{c}) - cdf^{\mathbf{o}(x,y)}(\mathbf{c}) \|^2 \mathrm{d}\mathbf{c}, \\ E_2 &= \int_\Phi \| \nabla(Ras(\mathbf{g}(x, y, L(\cdot)))) - \nabla(\mathbf{s}(x, y)) \|^2 \, \mathrm{d}x\mathrm{d}y. \end{aligned} \tag{5}$$

Here, $cdf(\cdot)$ denotes the cumulative distribution function; $\mathbf{o}(x, y)$ denotes the example image; Ω denotes the domain of colour space; ∇ denotes the gradient operator; Φ denotes the domain of pixel space and λ is a parameter to balance the influence of the two terms. The impact of λ is discussed in Section 5.1. Obviously, E_1 denotes the difference between the colour distributions of the transferred gradient mesh and the example image, and E_2 is the gradient constraint to preserve the details of the gradient mesh. Using the linear property in (3), E_1 and E_2 become

$$\begin{aligned} E_1 &= \int_\Omega \left\| cdf^{L(\mathbf{s}(x,y))}(\mathbf{c}) - cdf^{\mathbf{o}(x,y)}(\mathbf{c}) \right\|^2 \mathrm{d}\mathbf{c}, \\ E_2 &= \int_\Phi \| \nabla(L(\mathbf{s}(x, y))) - \nabla(\mathbf{s}(x, y)) \|^2 \, \mathrm{d}x\mathrm{d}y. \end{aligned} \tag{6}$$

Equation (6) means that we can faithfully formulate $L(\cdot)$ on the rasterized gradient mesh without rasterizing the edited gradient mesh multiple times.

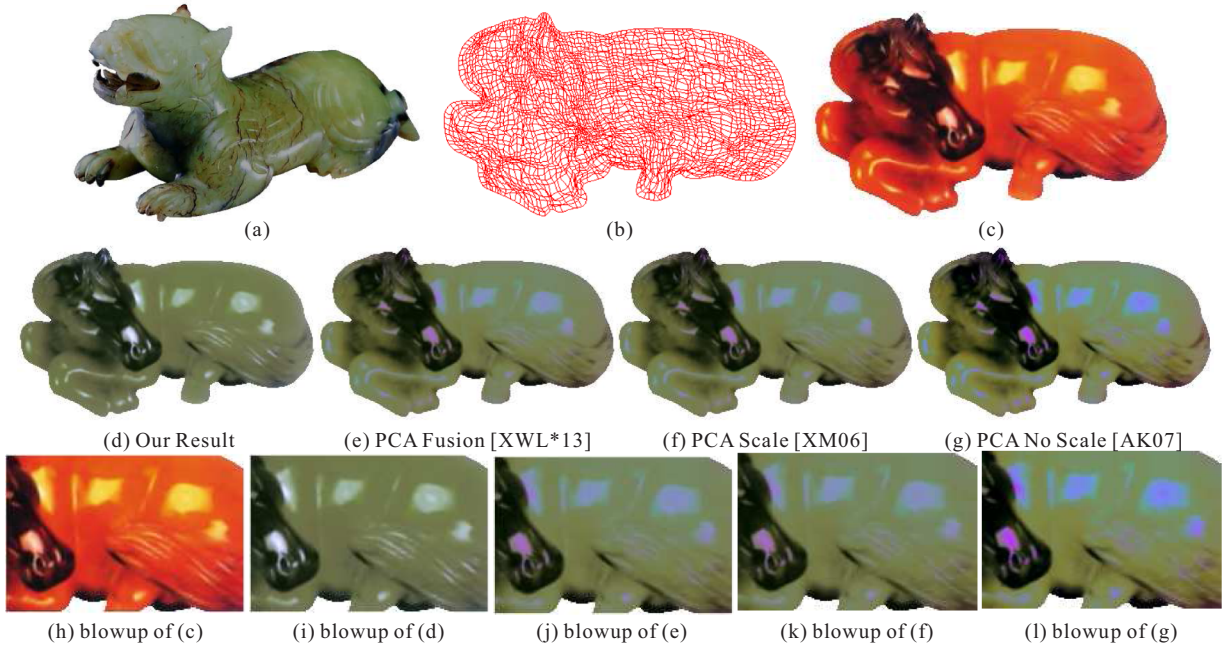

Figure 3: *Single-swatch colour transfer using different methods: (a) Reference image, (b) Mesh grids, (c) Rasterized gradient mesh, (d) Our result, (e) PCA fusion [XWL*13], (f) PCA with scaling and (g) PCA without scaling. Note that our result does not have abnormal colours and faithfully preserves the details of the gradient meshes. λ is set to 1 in this example.*

Since the $cdf(\cdot)$ functions in (6) are not differentiable and the calculation of the difference of the three-dimensional cdfs is computational intensive, previous methods often rely on random search to solve the problem [AP10], which is time-consuming. In fact, (6) can be efficiently approximated by first matching the colour distribution of the reference image $\mathbf{o}(x, y)$ and rasterized gradient mesh $\mathbf{s}(x, y)$, and then minimizing the difference of the linearly transferred colours and the matched colours. Since the distribution function of colours is three-dimensional, we adopt the N-dimensional probability distribution transfer method in [PKD07], which fully transfers the statistics of the reference image to the target images even in RGB space. After the distribution transfer, we obtain a set of reference colours $\mathbf{s}^{\mathbf{o}}(x, y)$, which almost have the same colour distribution as the example image $\mathbf{o}(x, y)$. Thereafter, E_1 can be approximated by

$$E_1' = \int_{\Phi} \|L(\mathbf{s}(x, y)) - \mathbf{s}^{\mathbf{o}}(x, y)\|^2 \, \mathrm{d}x\mathrm{d}y. \tag{7}$$

To summarize, our final energy function is given by

$$E' = \arg\min_{L} E_1' + \lambda E_2. \tag{8}$$

In (8), the functions of the unknown variables are linear in both the first and second terms. Therefore, T and $\mathbf{b}$ can be efficiently calculated from (8) by solving a linear system with only 12 variables. The detailed steps to solve T and $\mathbf{b}$ are given in the Supporting Information. After solving T and $\mathbf{b}$, we then transform the colours and colour gradients of the gradient mesh control points based on (2). The transformed colour vectors are given by

$$\mathbf{c}^l = T\mathbf{c}^t + \mathbf{b}, \tag{9}$$

where $\mathbf{c}^l$ denotes the transformed colour vector of a control point, $\mathbf{c}^t$ denotes the colour vector of a control point in the target gradient mesh. The transformed colour gradient vectors are given by

$$\begin{aligned} \mathbf{c}_u^l &= T\mathbf{c}_u^t, \\ \mathbf{c}_v^l &= T\mathbf{c}_v^t, \end{aligned} \tag{10}$$

where $\mathbf{c}_u^l$ and $\mathbf{c}_v^l$ denote the transformed colour gradient vector of a control point, $\mathbf{c}_u^t$ and $\mathbf{c}_v^t$ denote the colour gradient vector of a control point in the target gradient mesh.

Figure 3 shows an example in which the colour statistics of the image in Figure 3(a) are transferred to the gradient mesh in Figures 3(b) and (c). As a comparison, two PCA methods [XM06, AK07] which can be extended to gradient meshes are also used. As shown in Figure 3(d), our method faithfully captures the colour style of the example image, and also avoids abnormal colours, such as the purple colours in Figures 3(e)–(g), which are not present in the reference image 3(a). Moreover, our method better preserves the details of the original gradient mesh compared to the previous method [XWL*13] (see the highlights in the body and tail).

4.2. Multi-swatch colour transfer

When the single swatch method does not work well, we may choose separate colour swatch pairs and transfer desired colour effects between swatches [RAGS01]. This scheme can also provide more flexible user control of colour appearance. Our linear framework can be easily extended to multi-swatch colour transfer.

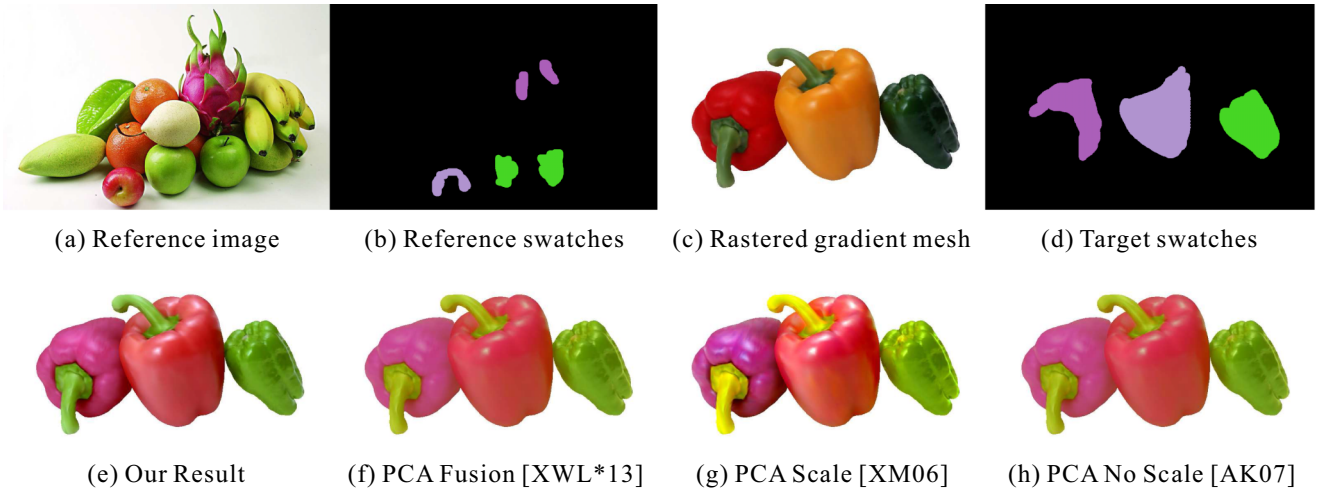

(a) Reference image (b) Reference swatches (c) Rastered gradient mesh (d) Target swatches

(e) Our Result (f) PCA Fusion [XWL*13] (g) PCA Scale [XM06] (h) PCA No Scale [AK07]

Figure 4: *Multi-swatch colour transfer using different methods. (a) Reference image, (b) Reference swatches, (c) Rasterized gradient mesh, (d) Target swatches, (e) Our result, (f) Result of PCA Fusion, (g) Result of PCA with scaling and (h) Result of PCA without scaling. Our result is more pleasing than the results of other methods. Note that a swatch pair is marked with the same colours. λ is set to 1 in this example.*

For the ith pair of swatches, we can obtain the transform matrix T_i and $\mathbf{b}_i$ using the single-swatch colour transfer method in Section 4.1. Then, the recoloured vectors will be a weighted sum of single-swatch recoloured vectors, given by

$$\begin{aligned} \mathbf{c}^l &= \sum_{i=1}^{M} w_i(T_i\mathbf{c}^t + \mathbf{b}_i), \\ \mathbf{c}_u^l &= \sum_{i=1}^{M} w_i T_i \mathbf{c}_u^t, \\ \mathbf{c}_v^l &= \sum_{i=1}^{M} w_i T_i \mathbf{c}_v^t, \end{aligned} \tag{11}$$

where M is the number of swatch pairs. The problem left is how to calculate the weighting factor w_is. Since weighting factors based on Mahalanobis distance have been shown to result in visually pleasing results [XWL*13], we choose to adopt this way to calculate w_is, given by

$$w_i = d_i / \sum_{j=1}^{M} d_j, \tag{12}$$

where d_i denotes the reciprocal of the Mahalonobis distance from a given colour c^t to a target colour swatch $I^t(i)$. d_i is given by

$$d_i = \frac{1}{\sqrt{(c^t - \eta_s(i))^T M_s(i)^{-1}(c^t - \eta_s(i))}}, \tag{13}$$

where $\eta_s(i)$ and $M_s(i)$ denote the mean vector and covariance matrix of swatch $I^t(i)$, respectively.

Figure 4 shows an example of using our multi-swatch colour transfer scheme. As shown in Figure 4(e), the colour style of the recoloured peppers is quite close to the reference swatches. Compared to our result, the results generated by [XWL*13, XM06, AK07] are obviously yellowish as shown in Figures 4(f)–(h), especially for the green pepper and the stems. Note that we transfer the colour of a light green apple to the dark green pepper. Moreover, our method better maintains the contrast of the gradient mesh because of the gradient constraint in our model.

Table 1: *User study repeated measures analysis.*

Similarity source	Type III sum of squares	df	Mean square	F	Sig
Method	57.31	3	19.10	16.65	0.00
Image group	1.27	4	0.32	0.62	0.65
Transition source	Type III sum of squares	df	Mean square	F	Sig
Method	94.89	3	31.63	28.50	0.00
Image group	3.82	4	0.95	2.46	0.053
Detail source	Type III sum of squares	df	Mean square	F	Sig
Method	69.26	3	23.09	24.72	0.00
Image group	1.40	4	0.35	0.72	0.58

5. Experimental Results

We generate gradient mesh vector graphics based on the algorithms from Sun *et al.* [SLWS07] and Lai *et al.* [LHM09]. For a given raster image, we first apply Lai *et al.*'s algorithm [LHM09] to create a gradient mesh automatically. If the quality of the rasterized gradient mesh is not very good, we optimize the gradient mesh using Sun *et al.*'s algorithm [SLWS07]. Note that [LHM09] extends the gradient mesh to tolerate image holes. To utilize [SLWS07], we decompose one hole-tolerated gradient mesh to two normal meshes at the hole. When the input image is complex, the image is segmented

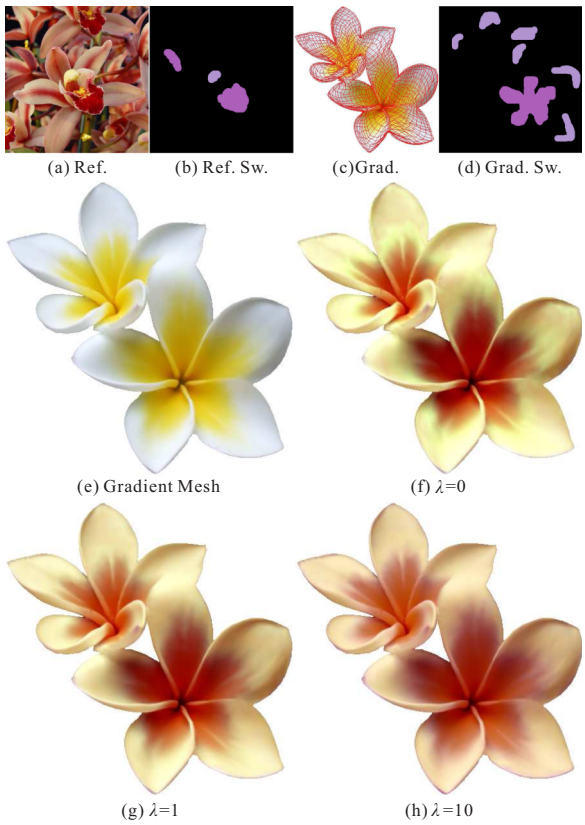

Figure 5: *The influence of λ on the results. (a) Reference image, (b) Reference swatches, (c) Gradient mesh, (d) Gradient mesh swatches, (e) Rasterized gradient mesh, (f) Result of* $\lambda = 0$*, (g) Result of* $\lambda = 1$*, (h) Result of* $\lambda = 10$*. As shown in (g), we obtain a good balance between the influence of the colour distribution term and gradient term by setting* $\lambda = 1$*.*

into several parts by manual or automatic methods [FH04, RKB04], and each part is approximated by one gradient mesh. Table 3 shows the number and size of the gradient meshes and the corresponding rasterized images used in the experiments.

5.1. The impact of λ

In our model (8), we use the parameter λ to balance the influence of the colour distribution term and the gradient term. In most of our experiments, we set $\lambda = 1$, which generates pleasing results in most cases. In this subsection, we use an example (Figure 5) to illustrate the impact of λ. As shown in Figure 5(f), when we only use the colour distribution term E_1' in (8), i.e. $\lambda = 0$, the recoloured result can faithfully capture the colour features of the reference swatches. However, some details of the original gradient mesh are destroyed, for instance the artefacts in the colour transition regions. When we use the gradient term as a constraint and set $\lambda = 1$, the artefacts are removed as shown in Figure 5(g). Further increasing λ can better preserve the details, but reduces the ability to match the colour distribution as shown in Figure 5(h).

5.2. Visual comparisons

Figures 1, 3, 4 and 6–8 show different examples recoloured by our method. Among the figures, the results in Figures 1, 3, 6 and 8 are generated by our single-swatch colour transfer method, and the others are generated by our multi-swatch colour transfer method. For the single-swatch colour transfer, no user input is required. For the multiple-swatch method, the only user intervention in our system is to specify the colour swatches. For example, in Figure 4, we use three pairs of colour swatches. Each pair of swatches is labelled with the same colour in the figure. In Figures 4 and 7, each of the three peppers is represented by a single gradient mesh, and just one colour swatch is specified for each pepper. For the purpose of comparison, we extend the two versions of the PCA method [XM06, AK07] to handle gradient mesh colour transfer in our experiments. The results of the PCA Fusion method [XWL*13] are also given.

As shown in these figures, although all the four methods can change the colour styles of the gradient mesh towards the reference images, the results of our method are visually more pleasing than those of PCA and PCA Fusion. In general, our method can faithfully capture the colour statistics of the reference images, avoid abnormal colours that are not present in the reference image and preserve the detail information of the gradient meshes. For instance, in the cloud example in Figure 6, the results of PCA Fusion and PCA with scaling have some green colours in the sky (see Figures 6e and f); the results of PCA without scaling have some blue colours in the sky (see Figure 6g). Neither the green colours nor the blue colours are present in the reference image (see Figure 6a). For the results of multi-swatch method, we can observe similar situations in Figure 7.

As mentioned in Section 1, the PCA Fusion method may cause some artefacts during the fusion step. Even if a gradient-preserving step [XWL*13] is applied to relieve the artefacts, they are still visible sometimes. As shown in Figure 8(f), the result of PCA Fusion has some extra textures which are not included in the original gradient mesh (see Figure 8a), while our result faithfully preserves the details (see Figure 8e).

5.3. Gradient mesh versus rasterized gradient mesh

In [XWL*13], the authors already pointed out the need to directly perform colour transfer on gradient meshes. Performing colour transfer on the rasterized gradient mesh and regenerating the gradient mesh not only consumes extra computing time, but also changes the structure of the gradient mesh. The changes in the structure are mainly caused by two reasons. First, the regenerating processes in [SLWS07, LHM09] are approximating operations, therefore, details of recoloured image will be blurred. Secondly, performing the colour transfer on the gradient mesh and its raster image may produce different results for multi-swatch colour transfer. In multi-swatch colour transfer, we sum the weighted result of single swatches. Since we process grid points or pixels separately, neighbouring grid points or pixels may have inconsistent weighting. For gradient meshes, they have their own structures which naturally avoid colour bleeding. That is, even inconsistent weighting in neighbouring grid points will generate smooth transitions. For the rasterized images of gradient meshes, this structure information is lost. Inconsistent weighting in neighbouring pixels on the raster image may

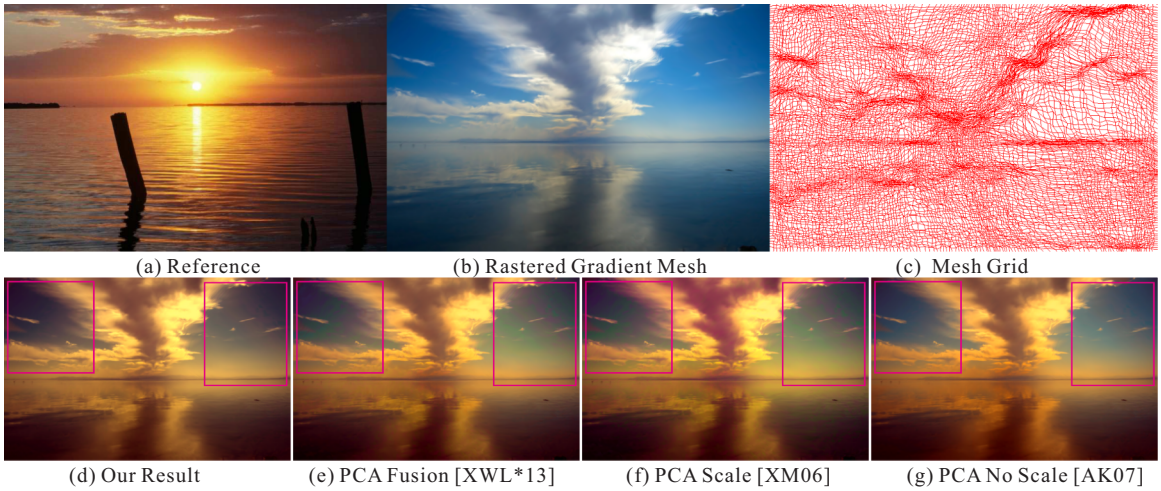

Figure 6: *Results of the cloud example. Note the unexpected green colours and blue colours in the highlighted regions of figures (e)–(g). The colour of our method is visually closer to the reference image. λ is set to 1 in this example.*

introduce obvious artefacts inside the inner regions of the gradient mesh patches. The artefacts can destroy the smooth transition of the gradient mesh. Figure 9 shows an example. In this figure, the black, yellow and light green colours are transferred to the orange, red and dark green peppers, respectively. As we can observe in Figure 9(e), there is an unexpected black band near the pepper stem. In contrast, the recoloured gradient mesh (Figure 9d) does not have such artefacts, and its colour transition remains as smooth as the original gradient mesh (Figure 9c). The reason for the artefacts is that the pixels in inner regions may be mapped to colours quite different from neighbouring pixels. This problem is more likely to appear when the swatches have quite different colours. For gradient meshes, only the colours and gradients of grid points are transformed, which guarantees inner regions have smooth transition.

5.4. User study

We conducted a user study to evaluate our method. Our user study consisted of a questionnaire given to 20 participants including 10 males and 10 females. Each questionnaire comprised 20 images, with five different images modified using four methods: our linear optimization method (LO for short) and three existing methods. The images were shown in a random order to each participant. Among them, five persons are artists working in design or other related areas. These people were asked to score each recoloured result image according to three criteria:

(1) Colour similarity between the result image and the example one. Since colours in the example image should be transferred, here we describe the colour similarity as the similarity of colour contrast or lighting ratio.
(2) Colour transition of the result image. Some methods may produce unnatural effects or introduce extra colours, and these kinds of artefacts would be expected to receive a low mark.
(3) Detail delineation of the result image. If a result image loses texture, or adds texture unreasonably, then its score would be lower.

Table 2: *User study LSD multiple comparisons.*

	Similarity Sig	Transition Sig	Detail Sig
LO versus PCAF	0.00	0.00	0.00
LO versus PCANS	0.00	0.00	0.00
LO versus PCAS	0.00	0.00	0.00
PCAF versus PCANS	1.00	0.38	0.07
PCAF versus PCAS	0.81	033	0.02
PCANS versus PCAS	0.76	0.08	0.00

Figure 10 shows the results of user study. There are five groups of images. The table under the bars list the average scores given by 20 participants. Note that each criterion has a five-point scale to evaluate the performance of different methods. The higher the score is, the better the result looks. The histogram illustrates the accumulated average scores of the three criteria. This graph informally indicates that people prefer the results of our method over the others.

For each criterion, we further analyse user study data by means of repeated measures analysis of variance (ANOVA). As listed in Table 1, the method type and the image group are the independent variables, and the user score is the dependent variable. We can see that the effect of the method type is significant, $F = 16.65$, Sig < 0.001 for colour similarity; $F = 28.5$, Sig < 0.001 for colour transition; $F = 24.72$, Sig < 0.001 for detail delineation. The effect of the image group, on the other hand, is not significant, since $F = 0.62$, Sig > 0.05 for colour similarity; $F = 2.46$, Sig > 0.05 for colour transition; $F = 0.72$, Sig > 0.05 for detail delineation. Furthermore, the least significant difference (LSD) multiple comparison among different methods in Table 2 shows that our method is significantly better than PCA Fusion [XWL*13], PCAS for PCA Scale [XM06] and PCANS for PCA No Scale [AK07], in terms of the three criteria, respectively. These three comparative methods have similar performance in terms of colour similarity and colour

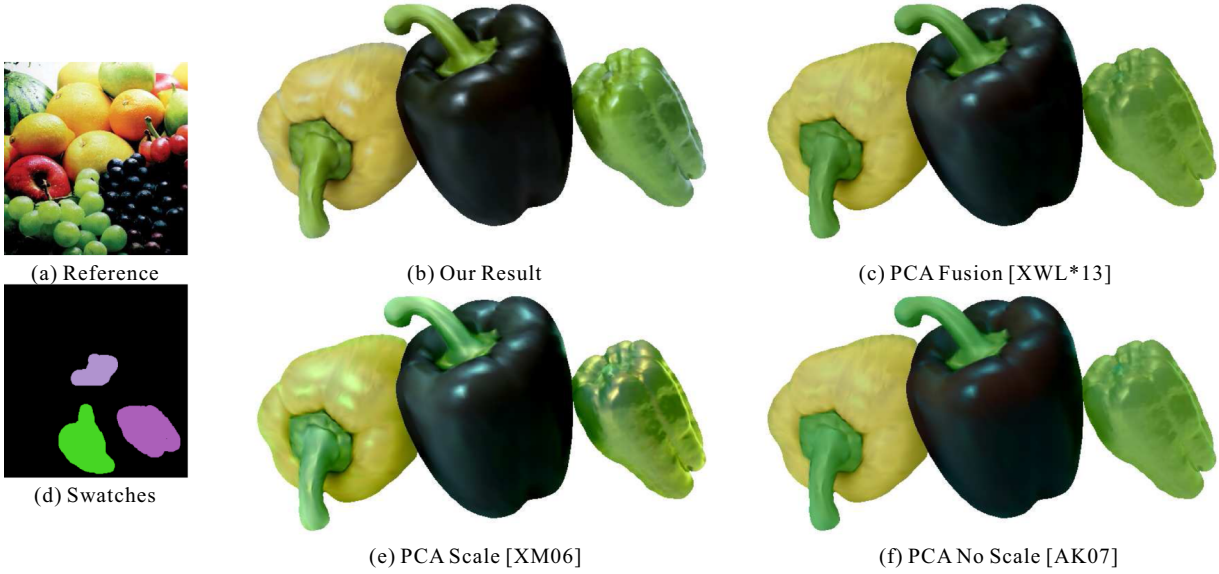

Figure 7: *Results of the peppers example: (a) Reference image; (b) Reference swatches; (c) Our Result; (d) Result of PCA Fusion [XWL*13]; (e) Result of PCA with scaling and (f) Result of PCA without scaling. Notice the colours of the green pepper, the stem and the highlight areas, the colours of our method are more similar to those of the reference image. The gradient mesh and its swatches are the same in Figure 4. Note that a swatch pair is marked with the same colours. λ is set to 1 in this example.*

Table 3: *The size of gradient meshes and the corresponding raster images used in the experiments.*

Name	Num.	Patches	Resolution
		28 × 13	
Jade (Figure 1)	3	28 × 8	600 × 450
Horse (Figure 3)	1	44 × 78	300 × 174
		30 × 33	
Peppers (Figure 4)	3	26 × 33	800 × 500
		38 × 63	
		37 × 32	
Plumeria (Figure 5)	2	37 × 30	446 × 456
Cloud (Figure 6)	1	126 × 127	800 × 511

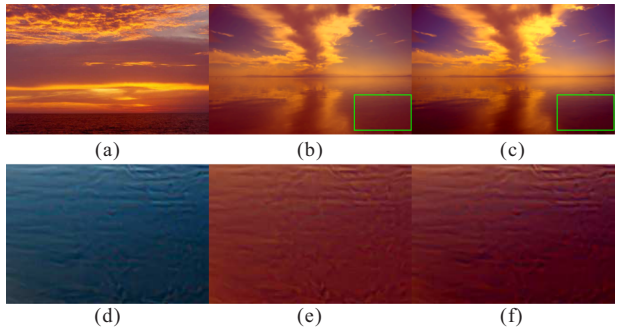

Figure 8: *Results of the cloud example: (a) Reference image; (b) Our Result; (c) Result of PCA Fusion [XWL*13]; (d) Blow-up of gradient mesh (enhanced); (e) Blow-up of our method (enhanced); (f) Blow-up of PCA Fusion (enhanced). The PCA Fusion method incurs small artefacts (extra textures), while our method has no such artefacts. Please view the digital images to observe the artefacts. The gradient mesh used in the same as in Figures 6(b)and (c). λ is set to 1 in this example.*

transition, while PCA Scale is significantly better than the other two with respect to detail delineation.

5.5. Time performance

We also evaluate the complexity and running time of our method. Our method is implemented using Matlab–C++ mixed programming. The N-dimensional probability distribution transfer and solving (8) are implemented in Matlab. They are compiled to DLL files, which are then called in our C++ interface. Since Matlab is not good at loop operation and extra time is spent on the data type conversion between Matlab and C++, our method is currently slower than the PCA Fusion method [XWL*13]. The running time of our method mainly depends on the time spent on the N-dimensional probability distribution transfer method [PKD07], solving (8), and performing (9) and (10). The first two parts are affected by the resolution of the rasterized gradient mesh, which are used for calculating the N-dimensional distribution matching and the gradient constraint. The computational complexity of the N-dimensional distribution transfer is $O(n)$ [PKD07], where n is the number of pixels in the rasterized gradient mesh. As we can see from the Supporting Information, the complexity to calculate the terms of the linear system is also $O(n)$. The complexity to solve the 12×12 linear system is $O(1)$. In performing (9) and (10), the complexity is $O(k)$, here k is

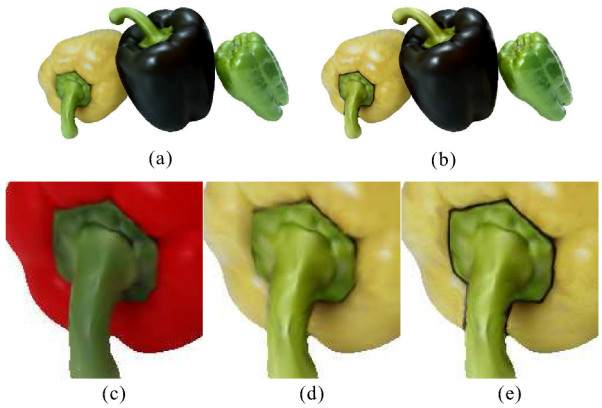

Figure 9: *Comparison between results on gradient mesh versus on raster images. (a) Result on gradient mesh, (b) Result on raster image, (c) Blow up of original gradient mesh, (d) Blow up of (a), (e) Blow up of (b). The swatches used are the same as those in Figure 7.*

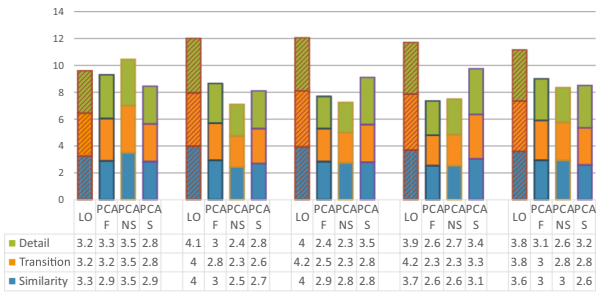

Figure 10: *Average scores of four methods. LO stands for our linear optimization method, PCAF for PCA Fusion [XWL*13], PCAS for PCA Scale [XM06] and PCANS for PCA No Scale [AK07]. From left to right, the image groups correspond to Figures 6, 3, 1, 4 and 7.*

the number of control points of the gradient mesh. The running time of our method is shown by parts in Table 4. In general, it takes our method at most 90 s for the examples in the experiments. The time difference between the raster images and the gradient meshes are not large. This is because the main time is spent on the N-dimensional probability distribution transfer and the solving (8).

If running speed is a concern, we can improve the speed of our method in several ways. One is to implement the Matlab part with C++. The other is to use a rasterized gradient mesh of smaller resolution for calculating the N-dimensional distribution matching and the gradient constraint. This can greatly improve the running speed with little impact on the recoloured image quality. Figure 11 shows an example. If we use a rasterized image of half width and half height, the run time of Parts 1 and 2 (defined in Table 4) are reduced from 20.28 and 71.75 to 10.14 and 17.79, respectively, while the recoloured results have no visual differences. The peak signal to noise ratio (PSNR) of these two results is 50.45. Another possible way is to use the GPU to accelerate the histogram-based operations in the N-dimensional distribution transfer as in [SH07].

Table 4: *Comparisons of running time (seconds) on gradient mesh and the corresponding raster image. 'Part 1' refers to the N-dimensional probability distribution transfer. 'Part 2' refers to solving (8). 'Part 3' refers to performing (9) and (10).*

	Gradient mesh			Raster image		
Part	1	2	3	1	2	3
Jade (Figure 1)	4.39	38.15	0.01	4.42	38.16	0.20
Horse (Figure 3)	1.95	7.87	0.02	2.20	8.20	0.05
Peppers (Figure 4)	2.37	12.97	0.16	2.38	13.14	3.68
Plumeria (Figure 5)	1.17	5.09	0.06	1.24	5.02	1.79
Cloud (Figure 6)	20.28	71.75	0.06	20.17	71.35	0.59

Figure 11: *Comparison of results using a smaller raster image. (a) The recoloured gradient mesh using a rasterized image whose resolution is* 800×511*.(b) The recoloured gradient mesh using a rasterized image whose resolution is* 400×256*. By using a raster image of half width and half height, the run time of Parts 1 and 2 (defined in Table 4) are reduced from 20.28 and 71.75 to 10.14 and 17.79, respectively. The PSNR of these two recoloured figures is 50.45. The example image and the gradient mesh are the same as in Figure 6.*

6. Limitations and Discussion

One limitation of our method is that finding a suitable reference image is sometimes difficult, which is the same as other colour transfer methods. Therefore, we would like to investigate more applications in our framework, which are more intuitive, such as colour theme enhancement [YP08, WYW*10], and scribble-based recolouring [LLW04]. Another limitation is that there is no standard way to choose an optimal λ in (8). It may require user tuning based on the visual effects. Nevertheless, pleasing results can be obtained by setting $\lambda = 1$ in most cases, as shown in the figures of this paper. In our current work, we focus on the linear transform, which makes use of the linear property of gradient meshes. In future work, we will also consider non-linear transforms for colour editing.

7. Conclusion

We have proposed an optimal linear operator for gradient meshes colour transfer. The colour transfer process is approximated by a linear operator solved from a minimization problem. The minimization problem explicitly considers both the colour statistics and the constraints to match the colour features and meanwhile avoid artefacts. The colours and colour gradients of control points in

gradient meshes are then transformed by the linear operator. The grid structure of the gradient mesh is preserved. The experimental results show that our method can generate pleasing recoloured gradient mesh.

Acknowledgements

We thank Prof. Xinyao Li at Sun Yat-Sen University for helping conducting the ANOVA analysis. The work was mainly supported by RGC General Research Fund from Hong Kong (Project No.: CityU 115612), and partially supported by the Fundamental Research Funds for the Central Universities (Project No.: 531107040842), Specialized Research Fund for the Doctoral Program of Higher Education, China (Project No.: 20110032120041), NSFC (Project No. 61272293), Shenzhen Nanshan Innovative Institution Establishment Fund (Project No. KC2013ZDZJ0007A) and Shenzhen Basic Research Project (Project No. JCYJ20120619152326448).

References

[AK07] Abadpour A., Kasaei S.: An efficient PCA-based color transfer method. *Journal of Visual Communication and Image Representation 18*, 1 (2007), 15–34.

[AP10] An X., Pellacini F.: User-controllable color transfer. *Computer Graphics Forum 29*, 2 (2010), 263–271.

[CHS08] Charpiat G., Hofmann M., Schölkopf B.: Automatic image colorization via multimodal predictions. In *Proceedings of the 10th European Conference on Computer Vision: Part III* (Marseille, France, 2008), vol. 5304, pp. 126–139.

[CSN03] Chang Y., Saito S., Nakajima M.: A framework for transfer colors based on the basic color categories. In *Proceedings of Computer Graphics International* (2003), pp. 176–181.

[CSN07] Chang Y., Saito S., Nakajima M.: Example-based color transformation of image and video using basic color categories. *IEEE Transactions on Image Processing 16*, 2 (2007), 329–336.

[DBZP10] Dong W., Bao G., Zhang X., Paul J.-C.: Fast local color transfer via dominant colors mapping. In *ACM SIGGRAPH ASIA Sketches* (2010), pp. 46:1–46:2.

[Fer64] Ferguson J.: Multivariable curve interpolation. *Journal of ACM 11*, 2 (1964), 221–228.

[FH04] Felzenszwalb P. F., Huttenlocher D. P.: Efficient graph-based image segmentation. *International Journal of Computer Vision 59* (2004), 167–181.

[FPC*14] Faridul H. S., Pouli T., Chamaret C., Stauder J., Tremeau A., Reinhard E.: A survey of color mapping and its applications. In *Eurographics State of the Art Report* (2014), pp. 43–67.

[GD05a] Grundland M., Dodgson N. A.: Color histogram specification by histogram warping. In *Proceeedings of the SPIE: Color Imaging X: Processing, Hardcopy, and Applications* (San Jose, CA, USA, 2005), vol. *5667*, pp. 610–621.

[GD05b] Grundland M., Dodgson N. A.: Color search and replace. In *Proceedings of the First Eurographics Conference on Computational Aesthetics in Graphics, Visualization and Imaging* (Girona, Spain, 2005), pp. 101–109.

[GH03] Greenfield G.-R., House D.-H.: Image recoloring induced by palette color associations. *Journal of WSCG 11*, 1 (2003), 189–196.

[HK05] Horiuchi T., Kotera H.: Colorization for monochrome image with texture. In *Proceedings of the 13th Color Imaging Conference* (Scottsdale, AZ, USA, 2005), pp. 245–250.

[HTC*05] Huang Y.-C., Tung Y.-S., Chen J.-C., Wang S.-W., Wu J.-L.: An adaptive edge detection based colorization algorithm and its applications. In *Proceedings of the 13th Annual ACM International Conference on Multimedia* (Hilton, Singapore, 2005), pp. 351–354.

[ICOL05] Irony R., Cohen-Or D., Lischinski D.: Colorization by example. In *Proceedings of the Sixteenth Eurographics Conference on Rendering Techniques* (Konstanz, Germany, 2005), pp. 201–210.

[JLWT04] Ji Y., Liu H.-B., Wang X.-K., Tang Y.-Y.: Color transfer to greyscale images using texture spectrum. In *Proceedings of International Conference on Machine Learning and Cybernetics* (Shanghai, China, Aug. 2004), vol. *7*, pp. 4057–4061.

[Kot05] Kotera H.: A scene-referred color transfer for pleasant imaging on display. In *Proceedings of IEEE International Conference on Image Processing* (Genoa, Italy, Sept. 2005), vol. *2*, pp. II–5–8.

[LHM09] Lai Y.-K., Hu S.-M., Martin R. R.: Automatic and topology-preserving gradient mesh generation for image vectorization. *ACM Transactions on Graphics 28*, 3 (2009), 1–8.

[LHZ08] Li J., Hao P., Zhang C.: Transferring colours to grayscale images by locally linear embedding. In *Proceedings of the British Machine Vision Conference* (Leeds, UK, 2008), pp. 83.1–83.10.

[LLW04] Levin A., Lischinski D., Weiss Y.: Colorization using optimization. *ACM Transactions on Graphics 23*, 3 (2004), 689–694.

[LWCO*07] Luan Q., Wen F., Cohen-Or D., Liang L., Xu Y.-Q., Shum H.-Y.: Natural image colorization. In *Proceedings of the 18th Eurographics Conference on Rendering Techniques* (Grenoble, France, 2007), pp. 309–320.

[LWX07] Luan Q., Wen F., Xu Y.-Q.: Color transfer brush. In *Proceedings of the 15th Pacific Conference on Computer Graphics and Applications* (Maui, Hawaii, 2007), pp. 465–468.

[MS03] Morovic J., Sun P.-L.: Accurate 3D image colour histogram transformation. *Pattern Recognition Letters 24*, 11 (2003), 1725–1735.

[MTN09] Morimoto Y., Taguchi Y., Naemura T.: Automatic colorization of grayscale images using multiple images on the web. In *SIGGRAPH: poster* (2009), pp. 59:1–59:1.

[NN05] Neumann L., Neumann A.: Color style transfer techniques using hue, lightness and saturation histogram matching. In *Proceedings of Computational Aesthetics in Graphics, Visualization and Imaging* (Girona, Spain, 2005), pp. 111–122.

[PKD07] Pitié F., Kokaram A. C., Dahyot R.: Automated colour grading using colour distribution transfer. *Computer Vision and Image Understanding 107*, 1–2 (2007), 123–137.

[PR11] Pouli T., Reinhard E.: Progressive color transfer for images of arbitrary dynamic range. *Computers and Graphics 35*, 1 (2011), 67–80.

[RAGS01] Reinhard E., Ashikhmin M., Gooch B., Shirley P.: Color transfer between images. *IEEE Computer Graphics and Applications 21*, 5 (2001), 34–41.

[RKB04] Rother C., Kolmogorov V., Blake A.: 'GrabCut': Interactive foreground extraction using iterated graph cuts. *ACM Transactions on Graphics 23*, 3 (2004), 309–314.

[RP11] Reinhard E., Pouli T.: Colour spaces for colour transfer. In *Proceedings of the Third International Conference on Computational Color Imaging* (Milan, Italy, 2011), pp. 1–15.

[SDYL12] Su Z., Deng D., Yang X., Luo X.: Color transfer based on multiscale gradient-aware decomposition and color distribution mapping. In *Proceedings of the 20th ACM International Conference on Multimedia* (Nara, Japan, 2012), pp. 753–756.

[SH07] Scheuermann T., Hensley J.: Efficient histogram generation using scattering on GPUs. In *Proceedings of the Symposium on Interactive 3D Graphics and Games* (Seattle, WA, USA, 2007), pp. 33–37.

[SLWS07] Sun J., Liang L., Wen F., Shum H.-Y.: Image vectorization using optimized gradient meshes. *ACM Transactions on Graphics 26*, 3 (2007), 11.

[TJT05] Tai Y.-W., Jia J.-Y., Tang C.-K.: Local color transfer via probabilistic segmentation by expectation-maximization. In *Proceedings of the IEEE Conference on Computer Vision and Pattern Recognition* (San Diego, CA, USA, 2005), vol. 1, pp. 747–754.

[WAM02] Welsh T., Ashikhmin M., Mueller K.: Transferring color to greyscale images. *ACM Transactions on Graphics 21*, 3 (2002), 277–280.

[WDM*11] Wu F., Dong W., Mei X., Zhang X. Jia X., Paul J.-C.: Distribution-aware image color transfer. In *SIGGRAPH Asia Sketches* (Hong Kong, China, 2011), pp. 8:1–8:2.

[WH04] Wang C. M., Huang Y. H.: A novel color transfer algorithm for image sequences. *Journal of Information Science and Engineering 20*, 6 (2004), 1039–1056.

[WHCO08] Wen C.-L., Hsieh C.-H., Chen B.-Y., Ouhyoung M.: Example-based multiple local color transfer by strokes. *Computer Graphics Forum 27*, 7 (2008), 1765–1772.

[WSM99] Weeks A. R., Sartor L. J., Myler H. R.: Histogram specification of 24-bit color images in the color difference (C-Y) color space. *Journal of Electronic Imaging 8*, 3 (1999), 290–300.

[WYW*10] Wang B., Yu Y., Wong T.-T., Chen C., Xu Y.-Q.: Data-driven image color theme enhancement. *ACM Transactions on Graphics 29*, 6 (2010), 146:1–146:10.

[XM06] Xiao X.-Z., Ma L.-Z.: Color transfer in correlated color space. In *Proceedings of the ACM International Conference on Virtual Reality Continuum and Its Applications* (Hong Kong, China, 2006), pp. 305–309.

[XM09] Xiao X.-Z., Ma L.-Z.: Gradient-preserving color transfer. *Computer Graphics Forum 28*, 7 (2009), 1879–1886.

[XWL*13] Xiao Y., Wan L., Leung C.-S., Lai Y.-K., Wong T.-T.: Example-based color transfer for gradient meshes. *IEEE Transactions on Multimedia 15*, 3 (2013), 549–560.

[YP08] Yang C.-K., Peng L.-K.: Automatic mood-transferring between color images. *IEEE Computer Graphics and Applications 28*, 2 (2008), 52–61.

[YS06] Yatziv L., Sapiro G.: Fast image and video colorization using chrominance blending. *IEEE Transactions on Image Processing 15*, 5 (2006), 1120–1129.

Supporting Information

Additional Supporting Information may be found in the online version of this article at the publisher's web site:

Figure S1: Comparison with the method in [RAGS01].

Figure S2: More results for additional gradient meshes.